AMERICAN SOCIETY FOR MICROBIOLOGY | Journal of Virology

Machupo Virus Expressing GPC of the Candid#1 Vaccine Strain of Junin Virus Is Highly Attenuated and Immunogenic

Takaaki Koma, Michael Patterson,* Cheng Huang, Alexey V. Seregin, Payal D. Maharaj, Milagros Miller, Jeanon N. Smith, Aida G. Walker, Steven Hallam, Slobodan Paessler

Department of Pathology, University of Texas Medical Branch at Galveston, Galveston, Texas, USA

ABSTRACT

Machupo virus (MACV) is the causative agent of Bolivian hemorrhagic fever. Our previous study demonstrated that a MACV strain with a single amino acid substitution (F438I) in the transmembrane domain of glycoprotein is attenuated but genetically unstable in mice. MACV is closely related to Junin virus (JUNV), the causative agent of Argentine hemorrhagic fever. Others and our group have identified the glycoprotein to be the major viral factor determining JUNV attenuation. In this study, we tested the compatibility of the glycoprotein of the Candid#1 live-attenuated vaccine strain of JUNV in MACV replication and its ability to attenuate MACV *in vivo*. Recombinant MACV with the Candid#1 glycoprotein (rMACV/Cd#1-GPC) exhibited growth properties similar to those of Candid#1 and was genetically stable *in vitro*. In a mouse model of lethal infection, rMACV/Cd#1-GPC was fully attenuated, more immunogenic than Candid#1, and fully protective against MACV infection. Therefore, the MACV strain expressing the glycoprotein of Candid#1 is safe, genetically stable, and highly protective against MACV infection in a mouse model.

IMPORTANCE

Currently, there are no FDA-approved vaccines and/or treatments for Bolivian hemorrhagic fever, which is a fatal human disease caused by MACV. The development of antiviral strategies to combat viral hemorrhagic fevers, including Bolivian hemorrhagic fever, is one of the top priorities of the Implementation Plan of the U.S. Department of Health and Human Services Public Health Emergency Medical Countermeasures Enterprise. Here, we demonstrate for the first time that MACV expressing glycoprotein of Candid#1 is a safe, genetically stable, highly immunogenic, and protective vaccine candidate against Bolivian hemorrhagic fever.

Machupo virus (MACV), which belongs to the *Arenaviridae* family, is the etiological agent of Bolivian hemorrhagic fever (BHF) (1). BHF was first identified in human patients in the Beni district of northeast Bolivia in 1959. More than 1,000 cases of BHF, of which 180 were fatal, were reported during an outbreak from 1962 to 1964 (2). Starting in 2006, after a long hiatus with no cases reported, the number of human cases steadily increased to more than 200 in 2008 (3). The clinical symptoms of BHF are similar to those of Argentine hemorrhagic fever (AHF), which is caused by Junin virus (JUNV). The case fatality rate of BHF is 25 to 35% (4, 5). Arenaviruses are enveloped, bisegmented (the L and S segments), negative-stranded RNA viruses (1). The L-segment genomic RNA encodes the RNA-dependent RNA polymerase L protein and the small zinc finger Z protein. The S segment encodes the viral nucleoprotein (NP) and the glycoprotein precursor (GPC) (1). The GPC is cleaved into the stable signal peptide (SSP) by signal peptidase and the mature glycoproteins GP1 and GP2 by the host subtilase subtilisin kexin isozyme-1/site 1 protease (SKI-1/S1P) (1, 6, 7). During arenavirus infection, the GPC on the surface of virus particles recognizes host receptors on the cell surface and mediates virus entry into the cells (8–11). The GPC of some arenaviruses might be a plausible target for prophylactic and therapeutic countermeasures against virus infection. For example, a Venezuelan equine encephalitis virus TC83 replicon vector expressing JUNV GPC provides efficient protection against JUNV infection in guinea pigs (12). Antibodies against JUNV GPC have been shown to neutralize JUNV infection in cultured cells (13).

Recently, Albarino et al. showed that the F427I substitution in the transmembrane domain (TMD) of GP2 of the attenuated Candid#1 (Cd#1) strain of JUNV was the critical attenuation factor in a suckling mouse model (14). Additionally, we have found that the F438I substitution in the TMD of MACV GP2, corresponding to the F427I change in the TMD region of Cd#1 GP2, attenuates MACV in alphabeta/gamma interferon receptor double-knockout (IFN-αβ/γ $R^{-/-}$) mice. However, the F438I mutation was unstable *in vivo*. MACV isolates reverting to the wild-type sequence (F438) were identified in mice that succumbed to MACV F438I infection (15). The importance of the F427I mutation in JUNV attenuation was also demonstrated in guinea pigs infected with JUNV. However, this mutation itself was apparently not sufficient to fully attenuate the virus; mild diseases and virus dissemination still occurred in these infected animals (16). In contrast, guinea pigs infected with a JUNV strain that expresses the

Received 12 October 2015 **Accepted** 2 November 2015

Accepted manuscript posted online 18 November 2015

Citation Koma T, Patterson M, Huang C, Seregin AV, Maharaj PD, Miller M, Smith JN, Walker AG, Hallam S, Paessler S. 2016. Machupo virus expressing gpc of the Candid#1 vaccine strain of Junin virus is highly attenuated and immunogenic. J Virol 90:1290–1297. doi:10.1128/JVI.02615-15.

Editor: S. Perlman

Address correspondence to Slobodan Paessler, slpaessl@utmb.edu.

* Present address: Michael Patterson, A&AS CBEP, Booz Allen Hamilton, Lorton, Virginia, USA.

whole GPC of Cd#1 origin did not develop symptoms and were protected against subsequent challenge with a virulent JUNV strain. As both MACV and JUNV belong to the clade B of the New World arenaviruses, in the present study, we tested the hypothesis that the Cd#1 GPC can replace the MACV GPC and attenuate MACV *in vivo*. To this end, we rescued a recombinant MACV strain expressing the entire GPC of Cd#1 (rMACV/Cd#1-GPC) and now report the *in vitro* and *in vivo* characterization of rMACV/Cd#1-GPC.

MATERIALS AND METHODS

Cells and viruses. Baby hamster kidney (BHK-21) cells (CCL-10; ATCC) were maintained in minimal essential medium (MEM; Life Technologies, Carlsbad, CA) supplemented with 10% fetal bovine serum (FBS; Life Technologies) and 1% penicillin-streptomycin (Life Technologies). Vero cells (CCL-81; ATCC) were maintained in Eagle's MEM with Earle's balanced salt solution and L-glutamine (Lonza, Basel, Switzerland) supplemented with 10% FBS (Life Technologies) and 1% penicillin-streptomycin (Life Technologies). A549 cells (CCL-185; ATCC) were maintained in Ham's F-12K medium (Life Technologies) containing 10% FBS (Life Technologies) and 1% penicillin-streptomycin (Life Technologies). Recombinant Cd#1 (rCd#1) (17), recombinant MACV strain Carvallo (rMACV) (18), and rMACV/Cd#1-GPC were rescued by using reverse genetics systems previously described. First-passage viruses were used for all infection experiments in this study. All work with infectious rMACV and rMACV/Cd#1-GPC was performed in the biosafety level 4 (BSL-4) laboratories at the Galveston National Laboratory (GNL), in accordance with the institutional safety guidelines.

Animal studies. Eight- to 15-week-old IFN-αβ/γ $R^{-/-}$ mice on a C57BL/6 background (strain 129 mice were backcrossed twice with C57BL/6 mice) were maintained in the animal BSL-2 (ABSL-2) and ABSL-4 facilities in GNL. All animal studies were reviewed and approved by the Institutional Animal Care and Use Committee at the University of Texas Medical Branch at Galveston. To evaluate the pathogenicity of rMACV, rCd#1, and rMACV/Cd#1-GPC, animals were challenged by intraperitoneal injection of each virus (10,000 PFU) and monitored for 42 days postinfection (dpi). Three animals per group were sacrificed at 17 dpi to evaluate viral dissemination in the infected animals. To study the protective efficacy of rMACV/Cd#1-GPC preimmunization against lethal MACV challenge, mice were immunized by intraperitoneal injection with phosphate-buffered saline (PBS), rCd#1, or rMACV/Cd#1-GPC (10,000 PFU) for 35 days and challenged by intraperitoneal injection of rMACV (10,000 PFU). Animals were humanely euthanized if they became moribund, if they lost more than 20% of their body weight, and/or if their body temperature fell below 34°C.

Construction of S segments for rMACV/Cd#1-GPC. The rMACV/Cd#1-GPC S segment with the MACV GPC gene replaced by the Cd#1 GPC gene was generated from three PCR amplicons by PCR. The three DNA segments were amplified from the pRF42-MACV S segment and the pRF42-Cd#1 S segment with the primers listed below (17, 18). The sequences of the primers (forward and reverse, respectively) were as follows: 5′-CGCACAGTGGATCCTAGGCAAAG-3′ and 5′-CCAACAGTTTGG CGTAGAGGACACTAAACACAGCCAAGACCCCTGCCGACCCG-3′ for the MACV NP side, 5′-CGGGTCGGCAGGGGTCTTGGCTGTGTT TAGTGTCCTCTACGCCAAACTGTTGG-3′ and 5′-GGTGTTGAAGT GTTGACACGCTCTCTAACACATGGGGCAGTTCATTAGCTTCATG CAAG-3′ for the Cd#1 GPC open reading frame part, and 5′-CTTGCAT GAAGCTAATGAACTGCCCCATGTGTTAGAGAGCGTGTCAACACT TCAACACC-3′ and 5′-CGCACCGGGGATCCTAGGCGATTC-3′ for the MACV GPC untranslated region (UTR) side. After digestion with AvrII and gel purification, the DNA of the rMACV/Cd#1-GPC S segment was inserted into the RNA polymerase I-driven expression plasmid pRF42 in an antigenomic orientation (17, 18).

Virus growth in cell culture and animals. To determine viral growth kinetics, Vero cells and A549 cells were infected at a multiplicity of infection (MOI) of 0.01, and the supernatant was collected from 0 to 96 h postinfection (hpi). To identify whether rMACV/Cd#1-GPC is genetically stable *in vitro*, we serially passaged the virus in Vero cells in duplicate as previously described (15). The serial passage was performed at an estimated MOI of 0.01 on the basis of the results in Fig. 1B. The viral titer in supernatants or in tissue homogenates was assessed by plaque assay on Vero cells as previously described (17, 19).

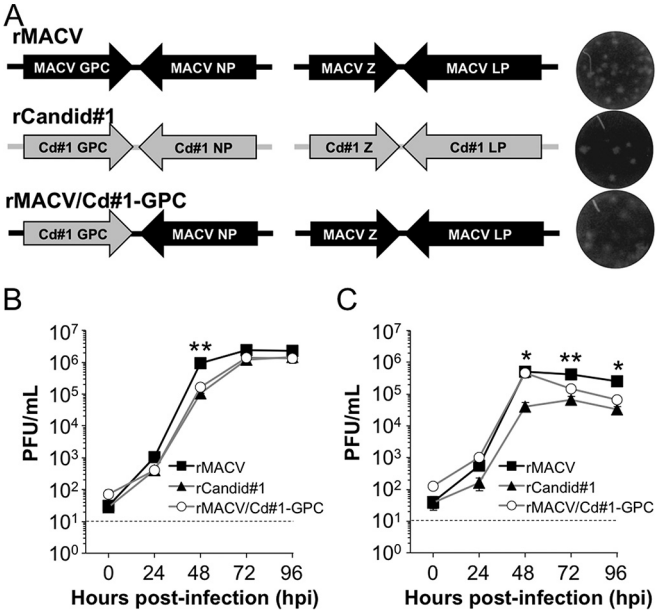

FIG 1 Schematic representation of the genome of rMACV/Cd#1-GPC and the virus growth curves. (A) For rMACV/Cd#1-GPC, the entire MACV GPC gene was replaced with the Cd#1 GPC gene. The plaque morphology is shown. (B) The growth of rMACV/Cd#1-GPC was characterized in Vero cells (MOI = 0.01). The titer of rMACV was significantly higher than that of rCd#1 at 48 hpi ($n = 5$; **, $P < 0.01$, based on one-way ANOVA with Dunnett's posttest comparing the groups to the Cd#1-infected group). The data shown are the averages ± SEMs from three experiments. (C) The growth of rMACV/Cd#1-GPC was characterized in A549 cells (MOI = 0.01). The titer of rMACV was significantly higher than that of rCd#1 at 48 hpi, 72 hpi, and 96 hpi, as well as the titer of rMACV/Cd#1-GPC at 48 hpi ($n = 4$; *, $P < 0.05$, based on one-way ANOVA with Dunnett's posttest comparing the groups to the Cd#1-infected group; **, $P < 0.01$, based on one-way ANOVA with Dunnett's posttest comparing the groups to the Cd#1-infected group). The data shown are the averages ± SEMs from two experiments. Dashed lines, the detection limit.

Measurement of virus-specific IgG titer by ELISA. To prepare antigens for enzyme-linked immunosorbent assay (ELISA), Vero cells were infected with rCd#1 at an MOI of 0.1 for 72 h. The infected cells were washed with PBS and lysed with cell lysis buffer (50 mM Tris-HCl, pH 8.0, 300 mM NaCl, 0.5% Triton X-100, 0.5% protease inhibitor cocktail [Sigma-Aldrich, St. Louis, MO]) on ice for 2 h and 30 min. After centrifugation, the supernatant was stored at −20°C. ELISA plates were coated with the 1:5-diluted cell lysate and incubated overnight at 4°C. The plates were washed three times with PBS containing 0.05% Tween 20 (PBS-T). After the plates were blocked with PBS-T containing 5% bovine serum albumin for 1 h at 37°C, 1:100-diluted serum samples were added to the plates and incubated for 1 h at 37°C. Next, the plates were washed with PBS-T and the bound antibody was detected with horseradish peroxidase-labeled goat anti-mouse IgG antibody (Southern Biotechnology, Birmingham, AL). Color reactions were performed with *o*-phenylenediamine dihydrochloride (OPD; Sigma-Aldrich) and allowed to develop for 20 min. The absorbance was measured at 450 nm using a VersaMax ELISA reader (Molecular Devices, Sunnyvale, CA).

PRNT. A plaque reduction neutralization test (PRNT) was performed on Vero cells as described previously (16). Briefly, 80 PFU of rMACV was

mixed with serially diluted heat-inactivated serum (final dilution range, 1:30 to 1:960) or medium. After incubation for 1 h at 37°C, the mixture was inoculated on Vero cells and incubated for 1 h at 37°C. Medium containing 0.6% tragacanth (Sigma) was used as an overlay. The titers are presented as the greatest serum dilution yielding a 50% reduction in plaque numbers ($PRNT_{50}$ titer).

RNA extraction and sequence analysis. To extract RNA, organs or cells were first suspended in the TRIzol reagent (Life Technologies). Organ tissue samples were homogenized using a TissueLyser system (Qiagen, Venlo, Netherlands) at 25 Hz for 5 min. RNAs were extracted using a Direct-zol RNA miniprep kit (Zymo Research, Irvine, CA) and reverse transcribed using a SuperScript III first-strand synthesis system (Life Technologies) and random primers according to the manufacturer's protocol. To determine the sequence of the viruses from organs or virus-infected cells (passages 1 to 5), cDNAs were amplified by PCR into two and three DNA fragments for viral S and L segments, respectively. The PCR products were purified using a QIAquick PCR purification kit (Qiagen) and directly sequenced using an ABI Prism 3130xl DNA sequencer (Life Technologies).

Determination of 5′ and 3′ UTRs of both S and L segments. The 5′ and 3′ UTRs of the S and L segments were determined by using a 5′ RACE system for rapid amplification of cDNA ends (RACE) and a 3′ RACE system for rapid amplification of cDNA ends, respectively (Life Technologies).

Histology. Tissues were collected from euthanized or dead animals and fixed in 10% buffered formalin for a minimum of 5 days. Then, the tissues were cut and embedded in paraffin, sectioned (5.0 μm), and stained with hematoxylin and eosin. For immunohistochemistry (IHC), the antigens were retrieved using 10× target retrieval solution (Dako Corp., Carpinteria, CA) for 45 min at 98°C. Endogenous peroxidase activity was blocked by incubation with 3% hydrogen peroxide in methanol for 30 min. A Histomouse-SP kit (Life Technologies) was used for IHC according to the manufacturer's protocol. The primary antibody added was monoclonal antibody (MAb) clone NA05-AG12 (1 μg/ml; incubation with the MAb was for 1 h with shaking at room temperature) that recognizes Junin virus NP and cross-reacts to MACV (13). A liquid diaminobenzidine substrate kit (Life Technologies) was used to visualize the virus antigens in the sections.

Statistical analysis. Data were analyzed using Dunnett's *post hoc* test following a one-way analysis of variance (ANOVA), log rank analysis, and the Mann-Whitney U test. Results were considered to be statistically significantly different when the P value was <0.05.

Nucleotide sequence accession number. The viral sequencing data for the S segment of rMACV/Cd#1-GPC were deposited in DDBJ/EMBL/GenBank (accession number LC066214).

RESULTS

Rescue and *in vitro* growth curve of rMACV/Cd#1-GPC. To test the compatibility of Cd#1 GPC with MACV, we designed the rMACV/Cd#1-GPC strain (Fig. 1A) in which the GPC gene in MACV genomic RNA was entirely replaced by the GPC gene from the live-attenuated Cd#1 strain of JUNV. rMACV/Cd#1-GPC was successfully rescued by using our reverse genetics system and characterized *in vitro*. The plaques formed by rMACV/Cd#1-GPC were similar in morphology to those formed by rMACV in Vero cells (Fig. 1A). However, at 48 hpi the growth of rMACV/Cd#1-GPC in cells was attenuated compared with that of rMACV and was the same as that of Cd#1 (Fig. 1B). The titers of all viruses eventually reached a similar highest level at 72 hpi. In human lung epithelial A549 cells, the titer of rMACV/Cd#1-GPC was identical to that of rMACV until 48 hpi, and then the virus titer was intermediate to the titers of rMACV and rCd#1 (Fig. 1C). To study the genetic stability of rMACV/Cd#1-GPC, we performed virus passaging studies in Vero cells in duplicate. After five passages in Vero cells, no mutation was found for the virus (data not shown).

***In vivo* characterization of rMACV/Cd#1-GPC.** It has been established that the Cd#1 GPC renders pathogenic JUNV avirulent in a mouse model and in guinea pigs (14, 16). To determine if Cd#1 GPC also renders MACV fully attenuated *in vivo*, rMACV/Cd#1-GPC was intraperitoneally inoculated into IFN-αβ/γ $R^{-/-}$ mice, which succumb to parental rMACV infection (18). Animals infected with rMACV started to lose more than 5% of their body weight at 10 to 18 dpi and developed disease symptoms, such as scruffy coats and hunched postures, at 11 to 15 dpi (Fig. 2B). These animals succumbed to infection at 24 to 35 dpi (Fig. 2A). Six of seven rMACV-infected animals exhibited hypothermia (body temperature, below 34°C) at 1 to 3 days prior to death, along with neurological manifestations, such as imbalance and paralysis (Fig. 2C). In contrast, no symptoms were observed in animals infected by rMACV/Cd#1-GPC or rCd#1.

To investigate virus dissemination, we collected brain, spleen, and liver tissue samples and serum samples from the infected animals. Three animals per group were euthanized at 17 dpi, while the remaining six or seven animals were euthanized at the terminal stage of the disease or at 42 dpi. Infectious virus was detected in all samples from animals infected with rMACV at all time points (Fig. 2D). The viral loads in the brains of terminally ill animals infected by rMACV were, on average, 170-fold higher than those at 17 dpi ($P < 0.05$ [Mann-Whitney U test]). However, the viral loads in the spleen, liver, and serum of rMACV-infected animals were similar at all time points. More importantly, no infectious virus was detected in the brain, spleen, and liver tissue samples and serum samples from rMACV/Cd#1-GPC- or rCd#1-infected animals.

To confirm viral infection in the animals, we tested serum samples for the presence of virus-specific IgG antibody using ELISA. All tested samples, except for one sample from an rCd#1-infected mouse collected at 17 dpi, were positive for virus-specific IgG (Fig. 2E). In addition, we detected neutralizing antibody against rMACV in some of these samples (Table 1). rMACV/Cd#1-GPC-infected animals developed high neutralizing antibody titers (geometric mean $PRNT_{50}$ titer, 161.5). In comparison, the neutralizing antibody titers were below the detection level in rMACV- and rCd#1-infected mice.

To investigate if the pathology changes were associated with infection, we performed histopathological and immunohistopathological examinations of the collected organs (Fig. 3). Pathological lesions were observed only in rMACV-infected animals. Occasional endothelial hypertrophy and vascular mononuclear infiltrates were present in the brains of rMACV-infected animals, and the virus antigen was broadly detected in the brain. Segregation of white and red pulp was disturbed in the spleens of rMACV-infected animals, while moderate microvesicular steatosis and mild perivascular mononuclear infiltrates were identified in the livers of rMACV-infected animals. No pathological changes were observed in either rMACV/Cd#1-GPC- or rCd#1-infected mice. Consistent with the pathology results, we were unable to detect viral RNA in the brains and spleens from rMACV/Cd#1-GPC- and rCd#1-infected mice at 17 dpi and 42 dpi. These results indicate that rMACV/Cd#1-GPC likely did not disseminate systemically or poorly disseminated systemically in mice.

rMACV/Cd#1-GPC inoculation induced protection against lethal MACV challenge. Since rMACV/Cd#1-GPC inoculation

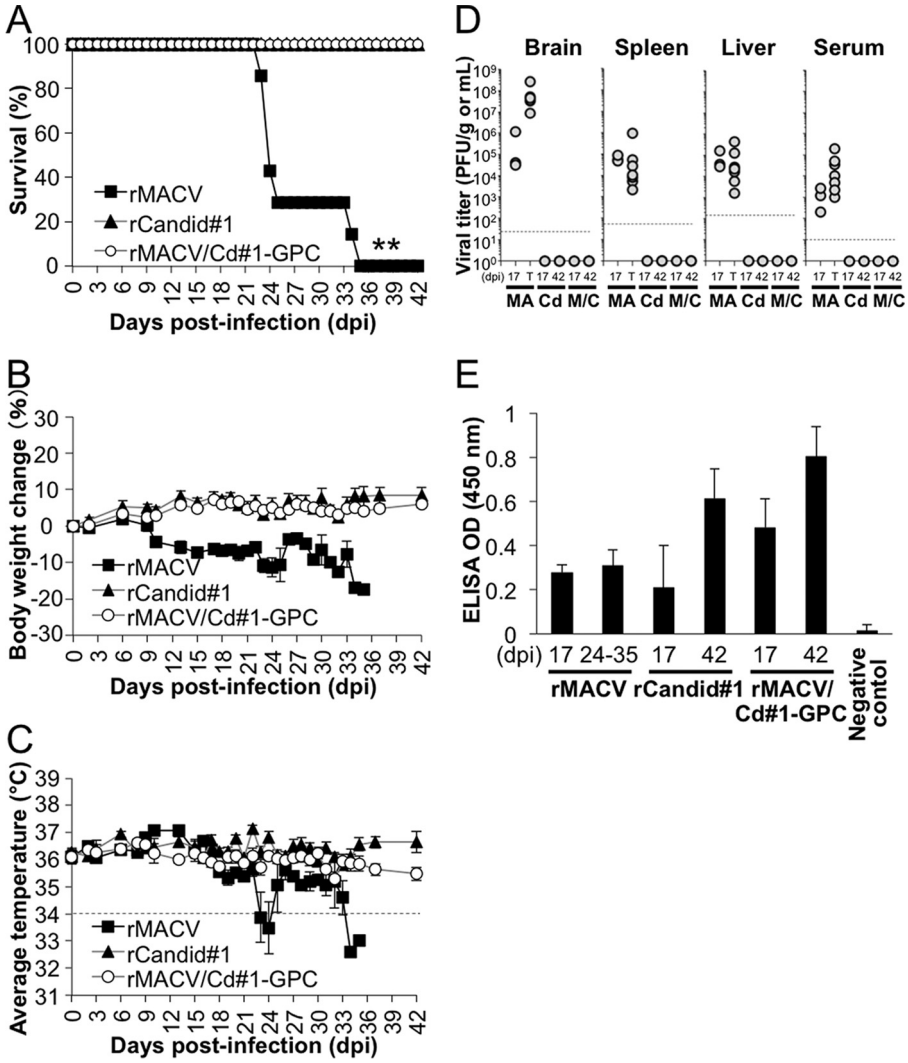

FIG 2 IFN-αβ/γ $R^{-/-}$ mice were infected with 10,000 PFU of rMACV/Cd#1-GPC, rMACV, or rCd#1 by the intraperitoneal route. (A) Survival curves of the infected mice ($n = 7$ for the rMACV/Cd#1-GPC- and rMACV-infected group; $n = 6$ for the rCd#1-infected group). **, $P < 0.01$ for the rMACV-infected group versus the rCd#1-infected group by log rank analysis. (B and C) Body weight (B) and body temperature (C) were monitored on the indicated days. All error bars indicate SEMs ($n = 7$ for the rMACV/Cd#1-GPC- and rMACV-infected group; $n = 6$ for the rCd#1-infected group). (D) Titers of rMACV/Cd#1-GPC, rMACV, and rCd#1 in tissues of infected mice at 17 dpi, the terminal stage (T; 24 to 35 dpi), and 42 dpi. The brains, spleens, and livers were harvested and homogenized. Organ tissue and serum samples were subjected to a plaque assay for virus titer. MA, rMACV; Cd, rCd#1; M/C, rMACV/Cd#1-GPC. Dashed line, the minimum detection limit. (E) To detect IgG antibody against the virus, rCd#1-infected cell lysate was used as the capture antigen. The bars show the mean optical density (OD) values plus SDs ($n = 3$ for 17 dpi, $n = 5$ for 24 to 42 dpi except for the rCd#1-infected group, for which $n = 4$). The optical density value obtained from uninfected cell lysates was used as the negative control for cell lysates and was subtracted from the data shown. Sera from 18 uninfected mice were used as the negative control for serum. A cutoff optical density value of 0.146 was defined as the mean +5 SDs for the negative control. All tested samples, except for one sample collected at 17 dpi (from the rCd#1-infected group), were positive. The data shown are pooled from two independent experiments.

induced high titers of neutralizing antibody against MACV, we tested the potency of its protection against MACV in this model. Animals were inoculated with rMACV/Cd#1-GPC, rCd#1, or PBS followed by challenge with a lethal dose of rMACV 35 days later. All rMACV/Cd#1-GPC-immunized mice survived the challenge without exhibiting signs of disease, while all rCd#1-immunized mice and PBS-immunized mice developed severe diseases with symptoms similar to those observed during MACV infection (Fig. 4A and B). Only one animal from each of these two groups survived; however, the two animals developed scruffy coats, a hunched posture, and hyperreflexia, all of which are indicative of suboptimal protection.

TABLE 1 $PRNT_{50}$ titer against rMACV after infection

$PRNT_{50}$ titer for the following group[a]:			
rMACV infected	rCd#1 infected	rMACV/Cd#1-GPC infected	Uninfected
<1:30 (35)	<1:30 (42)	1:120 (42)	<1:30
<1:30 (24)	<1:30 (42)	1:240 (42)	<1:30
<1:30 (24)	<1:30 (42)	1:60 (42)	<1:30
<1:30 (24)	<1:30 (42)	1:240 (42)	<1:30
<1:30 (25)	<1:30 (42)	1:240 (42)	
<1:30 (34)	<1:30 (42)	1:240 (42)	
<1:30 (23)		1:120 (42)	

[a] Numbers in parentheses are the day after infection.

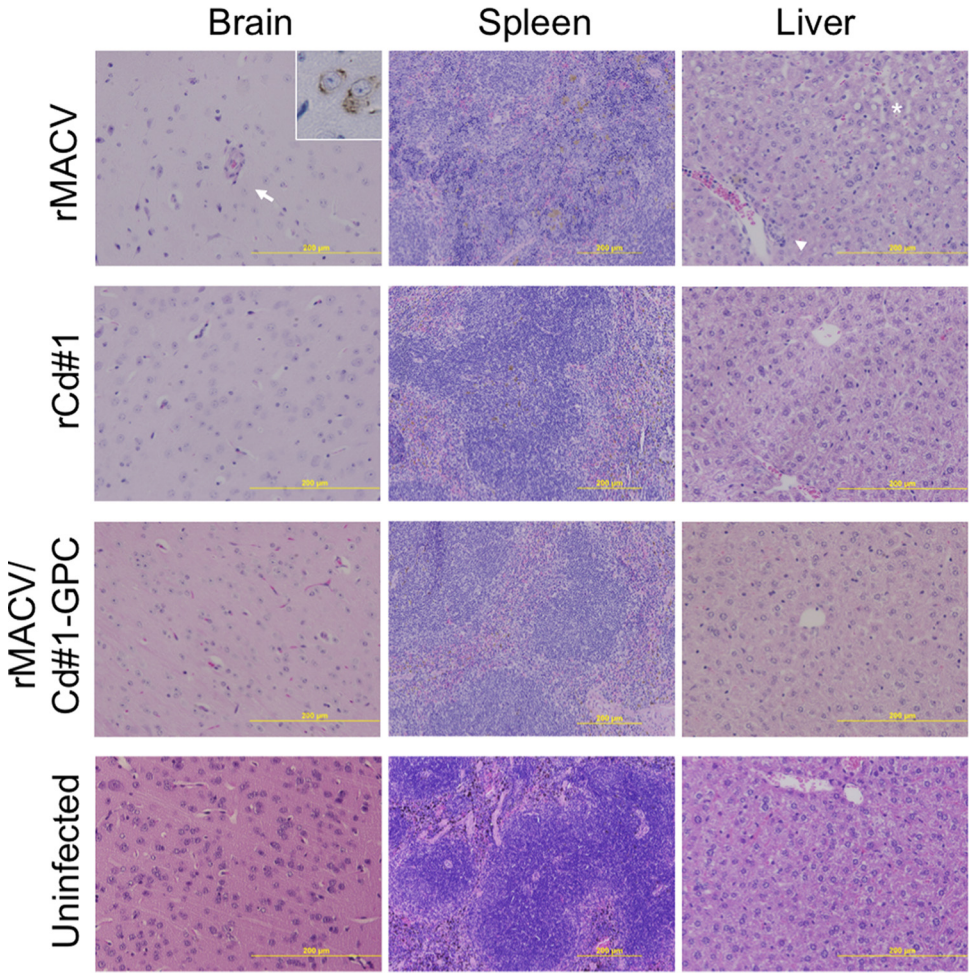

FIG 3 Histopathological changes in the brain, spleen, and liver from infected mice at the terminal stage or 42 dpi. In the cerebrum, virus antigen-positive cells were broadly detected in rMACV-infected animals (inset at top left; magnification, ×40) but were not detected in rCd#1- and rMACV/Cd#1-GPC-infected animals. Endothelial hypertrophy (arrow) and vascular mononuclear infiltrates were observed in the brains of rMACV-infected animals. Microvesicular steatosis (asterisk) and perivascular mononuclear infiltrates (arrowhead) were present in the livers of rMACV-infected animals. Magnifications, ×20 (brain and liver) and ×10 (spleen).

To determine the level of viral dissemination in preimmunized animals, viral loads were measured in mice that succumbed to the challenge or at 42 dpi (Fig. 4C). MACV was detected in all brain tissue and serum samples in the PBS-immunized group and in three of five brain tissue samples in the rCd#1-immunized group. In addition, three out of six PBS-immunized animals were positive for virus in the spleen and liver, while two of five rCd#1-immunized mice had infectious virus in the spleen, liver, and serum. Importantly, virus was not detectable in animals preimmunized with rMACV/Cd#1-GPC and challenged with rMACV.

The histopathological findings correlated with our virological findings and the outcome of infection: organs from animals preimmunized with rMACV/Cd#1-GPC had no detectable pathological changes (Fig. 5). On the other hand, mild to moderate lesions were observed in the brains, livers, and spleens of PBS-immunized and rCd#1-immunized animals.

Prior to rMACV challenge, neutralizing antibody against rMACV was detected only in the rMACV/Cd#1-GPC-immunized group (Table 2). After challenge, a substantial increase in the $PRNT_{50}$ titer was measured in the rMACV/Cd#1-GPC-immunized group. Two rCd#1-immunized mice developed higher $PRNT_{50}$ titers after challenge. Among the PBS-immunized mice, the level of neutralizing antibodies remained below the detection level in most animals after challenge and slightly increased in two animals.

DISCUSSION

In the present study, we utilized a reverse genetics system to successfully generate rMACV in which the GPC gene of MACV was replaced by that from the live-attenuated Cd#1 vaccine strain of JUNV. This is the first study to demonstrate the compatibility of the Cd#1 GPC with MACV. The resulting strain, rMACV/Cd#1-GPC, was fully attenuated in IFN receptor-knockout mice, an established mouse model of lethal MACV infection. Interestingly, a single immunization with rMACV/Cd#1-GPC was sufficient to completely protect mice from lethal rMACV infection. Our data showed that the Cd#1 GPC was compatible with the MACV GPC and efficiently supported the production of infectious MACV in cell culture. Both MACV and JUNV belong to clade B of the New

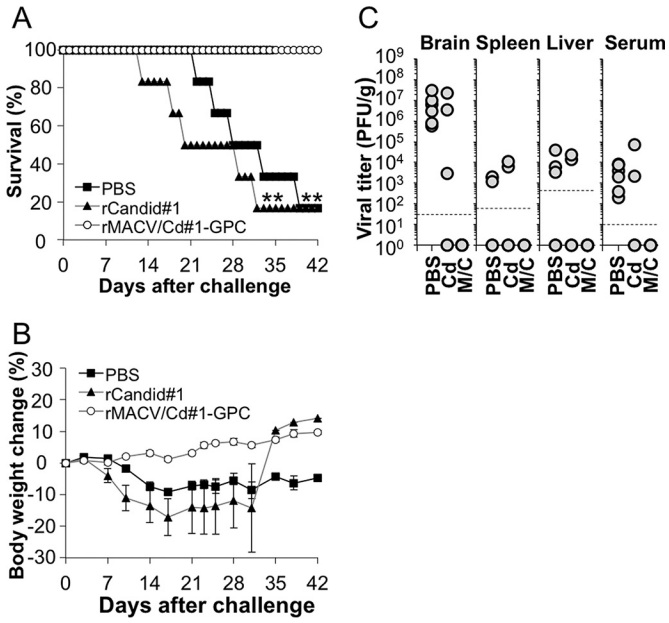

FIG 4 Mice were infected with rMACV at 35 days after immunization with rMACV/Cd#1-GPC, rCd#1, or PBS. (A) Survival curves for the infected mice ($n = 6$). **, $P < 0.01$ for rMACV/Cd#1-GPC- versus rCd#1-immunized mice and rMACV/Cd#1-GPC- versus PBS-immunized mice by log rank analysis. (B) Average body weight change (with SEM, $n = 6$) after rMACV challenge. (C) Virus titers in tissues of infected mice at the terminal stage (13 to 39 dpi) and 42 dpi. A plaque assay was performed for serum samples as well as for homogenized tissues from the brain, spleen, and liver. Cd, rCd#1; M/C, rMACV/Cd#1-GPC. Dashed lines, the minimum detection limit.

World arenaviruses (20). We have previously found that the L protein and NP from the Cd#1 strain of JUNV efficiently support MACV replication in a minigenome system, suggesting the feasibility of introducing viral genes from the attenuated JUNV into MACV (18). In Vero cells, the growth of rMACV/Cd#1-GPC seemed to be modestly delayed at 48 hpi, with the virus titer being approximately 10-fold lower than that of rMACV. rMACV/Cd#1-GPC eventually grew to titers similar to those of rMACV at 72 hpi. In A549 cells, the growth of rMACV/Cd#1-GPC was similar to that of rMACV until 48 hpi, and then the virus titer was intermediate to the titers of rMACV and rCd#1, demonstrating that overall there was no substantial impact on MACV production in infected cells when the MACV GPC gene was replaced with the Cd#1 GPC gene. However, we are not able to rule out the possibility that the attenuation of rMACV/Cd#1-GPC *in vivo* might be caused by a subtle incompatibility between Cd#1 GPC and other MACV structural proteins which might lead to the reduced infectivity of the chimeric virus. It is known that RNA viruses frequently undergo mutations in their genomes, which sometimes lead to phenotypic changes (21). Accordingly, we studied the genetic stability of rMACV/Cd#1-GPC by continuously passaging the virus in Vero cells a total of five times. No change in the entire viral genomic RNA sequence was identified, indicating a high degree of genetic stability for this recombinant virus. The high degree of genetic stability of rMACV/Cd#1-GPC also suggested that replacement of the MACV GPC gene with the GPC gene from the Cd#1 vaccine strain of JUNV did not affect the replication fitness of rMACV/Cd#1-GPC.

In addition, we found that introduction of the Cd#1 GPC gene into the MACV genome leads to the complete attenuation of MACV in a mouse model of lethal infection. This is in line with the findings of previous studies performed by others and us, in which GPC was identified to be the major viral factor for the attenuation of the vaccine strain of JUNV (14, 16, 22). Consistent with our previous report, rMACV infection was lethal to IFN-αβ/γ $R^{-/-}$ mice (15, 18). In contrast, the virological and pathological results clearly demonstrated that rMACV/Cd#1-GPC was avirulent in the IFN-αβ/γ $R^{-/-}$ mouse model, similar to the findings for the

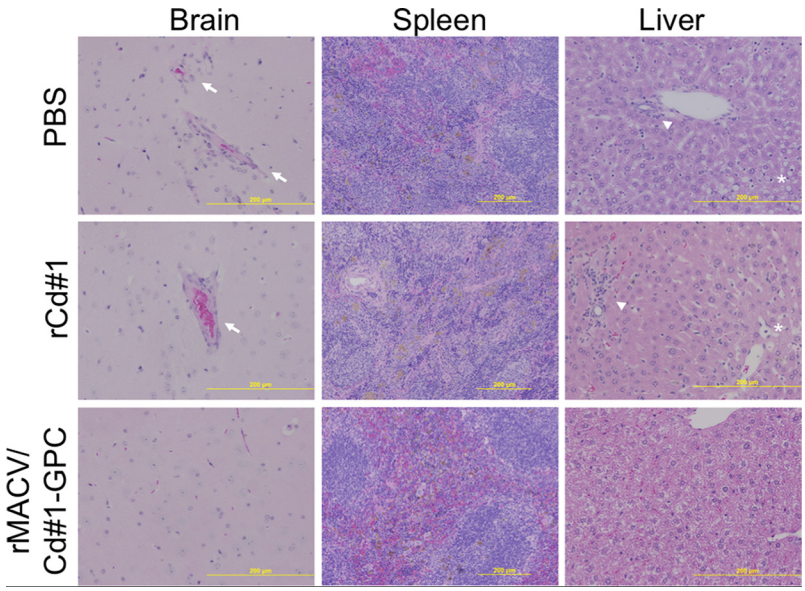

FIG 5 Histopathological changes in the brain, spleen, and liver from infected mice at the terminal stage or 42 days after challenge. Endothelial hypertrophy and vascular mononuclear infiltrates were observed in the brains of PBS-immunized animals and rCd#1-immunized animals (arrows). Microvesicular steatosis (asterisk) and perivascular mononuclear infiltrates (arrowheads) were observed in the livers of PBS-immunized animals and rCd#1-immunized animals. Magnifications, ×20 (brain and liver) and ×10 (spleen).

TABLE 2 $PRNT_{50}$ titer against rMACV pre- or postchallenge

$PRNT_{50}$ titer for the following group[a]:						
PBS treated		rCd#1 infected		rMACV/Cd#1-GPC infected		
Prechallenge[b]	Postchallenge	Prechallenge	Postchallenge	Prechallenge	Postchallenge	Uninfected
<1:30	<1:30 (25)	<1:30	NA[c] (20)	1:120	1:240 (42)	<1:30
<1:30	<1:30 (22)	<1:30	<1:30 (18)	1:120	1:240 (42)	<1:30
<1:30	<1:30 (28)	<1:30	NA (29)	1:60	1:240 (42)	<1:30
<1:30	1:60 (42)	<1:30	1:960 (32)	1:120	1:240 (42)	<1:30
<1:30	1:30 (33)	<1:30	NA (13)	1:60	1:60 (42)	
<1:30	<1:30 (39)	<1:30	1:480 (42)	1:30	1:960 (42)	

[a] Numbers in parentheses are the day after challenge.
[b] Prechallenge serum was collected at 35 days after immunization.
[c] NA, not available.

live-attenuated Cd#1 vaccine strain of JUNV. All animals survived without observable disease symptoms after intraperitoneal inoculation of rMACV/Cd#1-GPC. In rMACV/Cd#1-GPC- and Cd#1-infected mice, no infectious virus or viral RNA could be detected in the brain, spleen, liver, or serum at 17 dpi and 42 dpi, suggesting the possibility of limited or transient virus infection. However, further investigation is required to clarify whether the lack of detection of viral RNA and antigen in rMACV/Cd#1-GPC-infected mice at time points earlier than 17 dpi was attributable to antibody-mediated viral clearance or due to impaired viral multiplication of rMACV/Cd#1-GPC *in vivo*.

In addition to the complete attenuation of rMACV/Cd#1-GPC, we found that immunization with rMACV/Cd#1-GPC is highly immunogenic and elicits efficient protection against subsequent lethal challenge with the parental rMACV. While infectious virus or viral RNA could not be detected in rMACV/Cd#1-GPC-infected animals at the sample collection time points, the inoculation apparently induced a humoral immune response, as evidenced by the production of virus-specific IgG, as measured by ELISA. These data also suggested that the presumably restricted and/or transient infection of rMACV/Cd#1-GPC in animals was sufficient for induction of a host immune response. More importantly, rMACV/Cd#1-GPC immunization induced neutralizing antibodies, which likely contributed to the efficient protection of animals from lethal challenge with MACV. Although both rMACV/Cd#1-GPC and rCd#1 express the same Cd#1 GPC, it seems that rMACV/Cd#1-GPC is more immunogenic and protective than rCd#1. This was supported by the enhanced amount of anti-Cd#1 antibody production measured by ELISA (Fig. 2E), the strong neutralizing antibody resposne to MACV detected in the PRNT (Tables 1 and 2), and the efficacious protection against MACV challenge by rMACV/Cd#1-GPC but not by rCd#1 (Fig. 4). It is possible that rMACV/Cd#1-GPC might stimulate the host immune response more potently and/or might express viral antigens at higher levels than rCd#1 in mice. This possibility might explain the reason that rMACV/Cd#1-GPC eventually induced high neutralizing antibody responses to MACV (presumably against the GPC), in contrast to the findings for rCd#1. It is also worthy to note that rCd#1 infection efficiently induced neutralizing antibodies to Cd#1 in the PRNT (data not shown) but apparently not at a level sufficient to cross-protect from rMACV infection (Tables 1 and 2). The lysates used in the ELISA were prepared from rCd#1-infected cells and allowed the detection of antibodies to homologous GPC and NP of Cd#1, as well as the heterologous NP or GPC of MACV. Interestingly, the antibody levels in the rMACV/Cd#1-GPC-infected animals also appeared to be higher than those in the rCd#1-infected mice via ELISA analysis. Antibody-mediated immunity plays an important role in protection against infections by the New World arenaviruses, as immune plasma treatment with high levels of neutralizing antibody was effective in reducing the fatality rate from AHF in humans and BHF in nonhuman primates (NHPs) (23, 24). Therefore, higher humoral immune responses, likely along with cell-mediated responses, contribute to the efficacious protection elicited by rMACV/Cd#1-GPC but not rCd#1.

The antigenic cross-reactivity and cross-protection between the closely related MACV and JUNV have been previously characterized by other groups. Although some MAbs to JUNV GPC failed to cross-react to MACV GPC, as reported in one study (13), the MAb derived from mice immunized with MACV G2 recognized JUNV GPC in another study (25). Preliminary data reported at a conference showed that vaccination with Cd#1 was able to cross-protect against lethal MACV challenge in NHPs (26), suggesting the cross-neutralization between MACV and Cd#1 *in vivo*. In our mouse model, as well as in the NHPs described in the previous report (26), it is possible that not only the neutralizing antibodies but also the nonneutralizing antibodies as well as virus-specific $CD8^+$ T lymphocytes may contribute to the protection against lethal MACV challenge, as Cd#1 viremia often disappears before the appearance of measurable antibody in NHPs (27). Since homologous MACV NP, Z protein, and L protein are expressed by rMACV/Cd#1-GPC, presumably it might elicit a more potent $CD8^+$ T lymphocyte-mediated immune response against the NP, Z, and L proteins of MACV than against those of Cd#1. We found that the attenuation of rMACV/Cd#1-GPC was associated with its low infectivity and high immunogenicity in our animal model. This new finding could shed insight into the development of a MACV vaccine in the future.

In summary, we found that rMACV/Cd#1-GPC is fully attenuated in a mouse model of lethal infection. A single immunization with rMACV/Cd#1-GPC was highly immunogenic and elicited effective protection against rMACV challenge. More detailed and comprehensive studies are required to evaluate the pathogenicity of rMACV/Cd#1-GPC, as well as the mechanisms for its attenuation and immune protection. Our animal experiments involved the use of IFN-$\alpha\beta/\gamma$ $R^{-/-}$ mice. A study in animals with an intact interferon pathway, such as guinea pigs or NHPs, as recently described (28, 29), is required for the development of a safe and

efficacious vaccine against MACV infection. Our study also highlights the feasibility of attenuating other highly pathogenic New World arenaviruses, such as Guanarito virus, following the same approach by introducing the GPC gene from the Cd#1 vaccine strain of JUNV.

ACKNOWLEDGMENTS

This work was supported by Public Health Service grant R01AI093445 to S.P.

A.V.S. was supported by Biodefense Training Program, NIH, grant T32-AI060549.

FUNDING INFORMATION

HHS | NIH | National Institute of Allergy and Infectious Diseases (NIAID) provided funding to Slobodan Paessler under grant number R01AI093445. HHS | NIH | National Institute of Allergy and Infectious Diseases (NIAID) provided funding to Alexey V Seregin under grant number T32-AI060549.

REFERENCES

1. **Buchmeier MJ, de la Torre JC, Peters CJ.** 2007. Arenaviridae: the viruses and their replication, p 1791–1827. *In* Knipe DM, Howley PM, Griffin DE, Lamb RA, Martin MA, Roizman B, Straus SE (ed), Fields virology, 5th ed, vol 2. Lippincott Williams & Wilkins, Philadelphia, PA.
2. **Radoshitzky SR, de Kok-Mercado F, Jahrling P, Bavari S, Kuhn JH.** 2013. Bolivian hemorrhagic fever, p 339–358. *In* Singh S, Ruzek D (ed), Viral hemorrhagic fevers. CRC Press, Boca Raton, FL.
3. **Aguilar PV, Camargo W, Vargas J, Guevara C, Roca Y, Felices V, Laguna-Torres VA, Tesh R, Ksiazek TG, Kochel TJ.** 2009. Reemergence of Bolivian hemorrhagic fever, 2007-2008. Emerg Infect Dis **15:**1526–1528. http://dx.doi.org/10.3201/eid1509.090017.
4. **Charrel RN, de Lamballerie X.** 2003. Arenaviruses other than Lassa virus. Antiviral Res **57:**89–100. http://dx.doi.org/10.1016/S0166-3542(02)00202-4.
5. **Patterson M, Grant A, Paessler S.** 2014. Epidemiology and pathogenesis of Bolivian hemorrhagic fever. Curr Opin Virol **5:**82–90. http://dx.doi.org/10.1016/j.coviro.2014.02.007.
6. **Lenz O, ter Meulen J, Klenk HD, Seidah NG, Garten W.** 2001. The Lassa virus glycoprotein precursor GP-C is proteolytically processed by subtilase SKI-1/S1P. Proc Natl Acad Sci U S A **98:**12701–12705. http://dx.doi.org/10.1073/pnas.221447598.
7. **Nunberg JH, York J.** 2012. The curious case of arenavirus entry, and its inhibition. Viruses **4:**83–101. http://dx.doi.org/10.3390/v4010083.
8. **Abraham J, Kwong JA, Albarino CG, Lu JG, Radoshitzky SR, Salazar-Bravo J, Farzan M, Spiropoulou CF, Choe H.** 2009. Host-species transferrin receptor 1 orthologs are cellular receptors for nonpathogenic New World clade B arenaviruses. PLoS Pathog **5:**e1000358. http://dx.doi.org/10.1371/journal.ppat.1000358.
9. **Radoshitzky SR, Kuhn JH, Spiropoulou CF, Albarino CG, Nguyen DP, Salazar-Bravo J, Dorfman T, Lee AS, Wang E, Ross SR, Choe H, Farzan M.** 2008. Receptor determinants of zoonotic transmission of New World hemorrhagic fever arenaviruses. Proc Natl Acad Sci U S A **105:**2664–2669. http://dx.doi.org/10.1073/pnas.0709254105.
10. **Radoshitzky SR, Abraham J, Spiropoulou CF, Kuhn JH, Nguyen D, Li W, Nagel J, Schmidt PJ, Nunberg JH, Andrews NC, Farzan M, Choe H.** 2007. Transferrin receptor 1 is a cellular receptor for New World haemorrhagic fever arenaviruses. Nature **446:**92–96. http://dx.doi.org/10.1038/nature05539.
11. **Cao W, Henry MD, Borrow P, Yamada H, Elder JH, Ravkov EV, Nichol ST, Compans RW, Campbell KP, Oldstone MB.** 1998. Identification of alpha-dystroglycan as a receptor for lymphocytic choriomeningitis virus and Lassa fever virus. Science **282:**2079–2081. http://dx.doi.org/10.1126/science.282.5396.2079.
12. **Seregin AV, Yun NE, Poussard AL, Peng BH, Smith JK, Smith JN, Salazar M, Paessler S.** 2010. TC83 replicon vectored vaccine provides protection against Junin virus in guinea pigs. Vaccine **28:**4713–4718. http://dx.doi.org/10.1016/j.vaccine.2010.04.077.
13. **Sanchez A, Pifat DY, Kenyon RH, Peters CJ, McCormick JB, Kiley MP.** 1989. Junin virus monoclonal antibodies: characterization and cross-reactivity with other arenaviruses. J Gen Virol **70**(Pt 5):1125–1132. http://dx.doi.org/10.1099/0022-1317-70-5-1125.
14. **Albarino CG, Bird BH, Chakrabarti AK, Dodd KA, Flint M, Bergeron E, White DM, Nichol ST.** 2011. The major determinant of attenuation in mice of the Candid1 vaccine for Argentine hemorrhagic fever is located in the G2 glycoprotein transmembrane domain. J Virol **85:**10404–10408. http://dx.doi.org/10.1128/JVI.00856-11.
15. **Patterson M, Koma T, Seregin A, Huang C, Miller M, Smith J, Yun N, Smith J, Paessler S.** 2014. A substitution in the transmembrane region of the glycoprotein leads to an unstable attenuation of Machupo virus. J Virol **88:**10995–10999. http://dx.doi.org/10.1128/JVI.01007-14.
16. **Seregin AV, Yun NE, Miller M, Aronson J, Smith JK, Walker AG, Smith JN, Huang C, Manning JT, de la Torre JC, Paessler S.** 2015. The glycoprotein precursor gene of Junin virus determines the virulence of the Romero strain and the attenuation of the Candid #1 strain in a representative animal model of argentine hemorrhagic fever. J Virol **89:**5949–5956. http://dx.doi.org/10.1128/JVI.00104-15.
17. **Emonet SF, Seregin AV, Yun NE, Poussard AL, Walker AG, de la Torre JC, Paessler S.** 2011. Rescue from cloned cDNAs and in vivo characterization of recombinant pathogenic Romero and live-attenuated Candid #1 strains of Junin virus, the causative agent of Argentine hemorrhagic fever disease. J Virol **85:**1473–1483. http://dx.doi.org/10.1128/JVI.02102-10.
18. **Patterson M, Seregin A, Huang C, Kolokoltsova O, Smith J, Miller M, Smith J, Yun N, Poussard A, Grant A, Tigabu B, Walker A, Paessler S.** 2014. Rescue of a recombinant Machupo virus from cloned cDNAs and in vivo characterization in interferon (alphabeta/gamma) receptor double knockout mice. J Virol **88:**1914–1923. http://dx.doi.org/10.1128/JVI.02925-13.
19. **Kolokoltsova OA, Grant AM, Huang C, Smith JK, Poussard AL, Tian B, Brasier AR, Peters CJ, Tseng CT, de la Torre JC, Paessler S.** 2014. RIG-I enhanced interferon independent apoptosis upon Junin virus infection. PLoS One **9:**e99610. http://dx.doi.org/10.1371/journal.pone.0099610.
20. **Koma T, Huang C, Kolokoltsova OA, Brasier AR, Paessler S.** 2013. Innate immune response to arenaviral infection: a focus on the highly pathogenic New World hemorrhagic arenaviruses. J Mol Biol **425:**4893–4903. http://dx.doi.org/10.1016/j.jmb.2013.09.028.
21. **Domingo E, Holland JJ.** 1997. RNA virus mutations and fitness for survival. Annu Rev Microbiol **51:**151–178. http://dx.doi.org/10.1146/annurev.micro.51.1.151.
22. **Droniou-Bonzom ME, Reignier T, Oldenburg JE, Cox AU, Exline CM, Rathbun JY, Cannon PM.** 2011. Substitutions in the glycoprotein (GP) of the Candid#1 vaccine strain of Junin virus increase dependence on human transferrin receptor 1 for entry and destabilize the metastable conformation of GP. J Virol **85:**13457–13462. http://dx.doi.org/10.1128/JVI.05616-11.
23. **Maiztegui JI, Fernandez NJ, de Damilano AJ.** 1979. Efficacy of immune plasma in treatment of Argentine haemorrhagic fever and association between treatment and a late neurological syndrome. Lancet **ii:**1216–1217.
24. **Eddy GA, Wagner FS, Scott SK, Mahlandt BJ.** 1975. Protection of monkeys against Machupo virus by the passive administration of Bolivian haemorrhagic fever immunoglobulin (human origin). Bull World Health Organ **52:**723–727.
25. **York J, Berry JD, Stroher U, Li Q, Feldmann H, Lu M, Trahey M, Nunberg JH.** 2010. An antibody directed against the fusion peptide of Junin virus envelope glycoprotein GPC inhibits pH-induced membrane fusion. J Virol **84:**6119–6129. http://dx.doi.org/10.1128/JVI.02700-09.
26. **Jahrling P, Trotter R, Barrero O.** 1988. Crossprotection against Machupo virus with Candid 1 Junin virus vaccine, p E3. Abstr 2nd Int Conf Impact Viral Dis Dev Latin Am Countries Caribbean Region, Mar del Plata, Argentina.
27. **McKee KT, Jr, Oro JG, Kuehne AI, Spisso JA, Mahlandt BG.** 1993. Safety and immunogenicity of a live-attenuated Junin (Argentine hemorrhagic fever) vaccine in rhesus macaques. Am J Trop Med Hyg **48:**403–411.
28. **Bell TM, Bunton TE, Shaia CI, Raymond JW, Honnold SP, Donnelly GC, Shamblin JD, Wilkinson ER, Cashman KA.** 2 July 2015. Pathogenesis of Bolivian hemorrhagic fever in guinea pigs. Vet Pathol. http://dx.doi.org/10.1177/0300985815588609.
29. **Bell TM, Shaia CI, Bunton TE, Robinson CG, Wilkinson ER, Hensley LE, Cashman KA.** 2015. Pathology of experimental Machupo virus infection, Chicava strain, in cynomolgus macaques (Macaca fascicularis) by intramuscular and aerosol exposure. Vet Pathol **52:**26–37. http://dx.doi.org/10.1177/0300985814540544.